

Contour Extraction Based on Deformable Model and Dynamic Programming

Zhao Cheng^{*}

Institute of Manned Space System Engineering, China Academy of Space Technology, Beijing 100094, China; Email: 3254059705@qq.com.

Keywords: deformable model, region of interest, dynamic programming, contour extraction

Abstract. In this paper, a new model for extraction of active contours of the quasi-circular targets in a given image which is based on edge detection and dynamic programming (DP) is proposed. In order to guarantee the detected closed contour approximating to the real contour of the target as well as possible, the DP algorithm was launched as the probability distribution of the polar image's edge is obtained by which the computational time was significantly reduced. By the utilization of the image intensity information and the balloon force, the external force in the energy-minimizing function of deformable model is synthetically designed. The theoretical analysis and experiment results demonstrated that the capability of searching a continuous and closed edge contour with the proposed method was remarkably extended compared to the other two methods.

1. Introduction

The traditional Snake was first introduced by Kass et al. in 1988. Some methods[1] have been proposed to solve this problem, including finite element method, DP algorithm[2-3], greedy algorithm. For example, Amini et al.[4] use the time delayed discrete dynamic programming method to solve the energy minimization problem defined by the ACM. In 2006, H. Zhang et al. [5] propose an automated tongue segmentation method via combining polar edge detector and active contour model. Collewet[6] used a polar description based on orthogonal functions as the parametric curve to describe the contour and introduced an external force derived from an energy term based on the area inside the contour. A detailed investigation on above-mentioned problems is made in this paper, based on which a novel edge extraction method for quasi-circular targets based on deformable model and dynamic programming was designed. The outline of this paper is as follows: The overall contour extraction of targets framework is presented in Section 2, and Section 2 contains edge detection under polar coordinates and building of energy function. In Section 3, we describe the extraction of closed edge contour by using DP. Section 4 shows some experimental results, and the work is summarized and future work is discussed in Section 5.

2. Deformable Model

Deformable model mainly consists of two parts: edge information detection and dynamic programming algorithm. Edge information may provide fundamental knowledge for parameterized deformable model, and also prepare for launching DP to obtain optimum, clear, continuous and closed contour. Fig. 1 shows the flow chart of the proposed method.

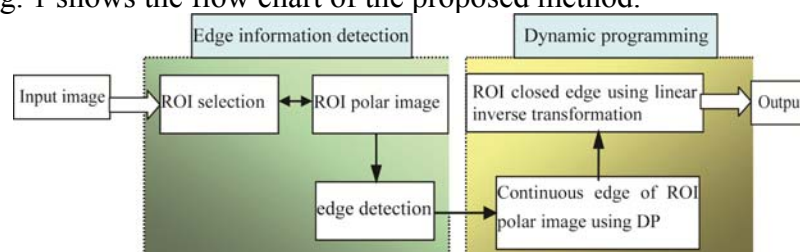


Fig. 1 The flow chart of the proposed method

2.1 Edge Detection.

Fig. 2(a) is a mammogram with benign mass (come from [7]). As showed in Fig. 2, we select a point in mass region and draw the ROI. The blue point is the center point (C_x, C_y) and R is the radius of ROI in Fig. 2(b).

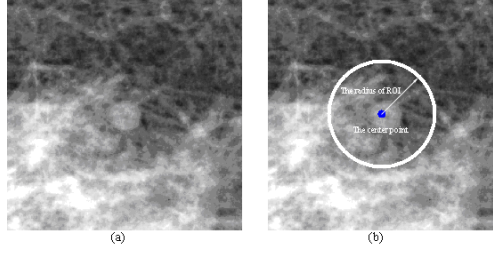


Fig. 2 (a)Mammogram with benign mass (b)Region of interest

We render the center of ROI as the origin of the polar coordinate system $O(r, \theta)$ with the following conditions:

$$\begin{cases} x = r \cos \theta \\ y = r \sin \theta \end{cases}, \quad 0 \leq r \leq R, 0 \leq \theta \leq 2\pi. \quad (1)$$

The ROI $I(x, y)$ shown in Cartesian coordinates was transformed into polar image $I'(x, y)$.

2.2 Engergy Function.

For a discrete digital image, when it was modeled as a polar image, the radius r and the polar angle θ can be quantificated with an equidistant interval, and then we can have:

$$\begin{cases} r_i = i \times (R/M), & i = 0, 1, 2, \dots, M-1 \\ \theta_j = j \times (R/N), & j = 0, 1, 2, \dots, N-1 \end{cases} \quad (2)$$

Thus, a discrete grid or matrix whose sizes are $M \times N$ is obtained. To describe the algorithm in a brief way, $r_i(\theta_j)$ is denoted as $r_{i,j}$ for short, and we denote any point $q(r_i, \theta_j)$ on the grid as q_j similarly as a result of arrangement orderly for candidate points of contour. The optimal path can be expressed with a broken line $B_N^* = \{q_1^*, q_2^*, \dots, q_N^*, q_1^*\}$, which is composed from a candidate point q_1^* on the first column of matrix to q_N^* on the last column along the polar angle direction, and come back to q_1^* at last. The broken line has minimum energy $E(B_N^*)$, and it also represents the continuous edge curve of polar image.

In the Snake model, the local energy of any point q_j or $q_{j-1}q_j$ on the mesh is expressed:

$$E(q_j) = E_{\text{int}}(q_j) + E_{\text{im}}(q_j) + E_{\text{ext}}(q_j) \quad (3)$$

where $E_{\text{int}}(q_j)$ is defined as internal energy as follows:

$$E_{\text{int}}(q_j) = \alpha(q_j) |\gamma_{i,j} - \gamma_{k,j-1}| + \beta(q_j) |\gamma_{i,j} - \gamma_{k,j-1}| |r_{i,j} + r_{k,j-1}| \frac{2\pi}{N} \quad (4)$$

where $\alpha(q_j)$ and $\beta(q_j)$ represent parameters of the point q_j separately. E_{im} represents the potential energy result from image force, in which we adopt the normalized gradient magnitude, and it is defined as:

$$E_{\text{im}}(q_j) = \gamma(q_j) \cdot (1 - g(q_j)). \quad (5)$$

E_{ext} is denoted as external energy which is constituted of the resultant force of the gray external force and the geometric expansive force, which is defined as:

$$E_{\text{ext}}(q_j) = \mu(q_j) \cdot |\text{gray}(q_j) - \text{gray}(q_{j-1})| + \sigma(q_j) \cdot (r_{i,j} + r_{k,j-1})^2 \cdot \frac{2\pi}{N} \quad (6)$$

Where $\mu(q_j)$ and $\sigma(q_j)$ represent the parameters of the point q_j , and $\text{gray}(q_j)$ represents the gray intensity of the point q_j . Design of the external energy E_{ext} is a crucial step in our method for it has a direct impact on the choice of the control points. The details were given as following:

(1) For an image containing quasi-circular targets, it can be divided into three regions: target internal region, background region and target marginal region in which the real contour was involved. When the target ROI was built by (C_x, C_y) as the centre of circle and R as the radius. For example, the points subject to $|x - c_x|^2 + |y - c_y|^2 \leq \delta_1$ are regarded as target internal region approximately, and the ones restrict to $\delta_2 \leq |x - c_x|^2 + |y - c_y|^2 < R$ belong to background region roughly, where δ_1, δ_2 are epsilons. By which the gray mean m_{int} and the standard deviation σ_{int} of target internal area, the gray mean m_{back} and the standard deviation σ_{back} of background area can be obtained. What should be stressed is that, prior to the calculation of m_{int} or σ_{back} etc., only the middle part of the ordered gray value was reserved to eliminate the effect of noise. Then, several rings can be got when the target centroid coordinate (C_x, C_y) approximately is regard as center of concentric circles.

(2) According to position of two adjacent control points located in ROI, the dynamic design of the direction of parameters $\mu(q_j), \sigma(q_j)$ in energy term E_{ext} is shown as follows:

(a) When q_{j-1} locates in background area where it contents with $m_{back} - 3\sigma_{back} \leq \text{gray}(q_{j-1}) \leq m_{back} + 3\sigma_{back}$, and q_j locates in target internal area depended on $m_{int} - 3\sigma_{int} \leq \text{gray}(q_j) \leq m_{int} + 3\sigma_{int}$, we set $\mu(q_j) := -\mu(q_{j-1}); \sigma(q_j) := \sigma(q_{j-1})$. (b) When q_{j-1} locates in target internal area and q_j locates in background area, we set $\mu(q_j) := -\mu(q_{j-1}); \sigma(q_j) := \sigma(q_{j-1})$. (c) When q_{j-1} and q_j are both locate in target internal area, we set $\mu(q_j) := \mu(q_{j-1}); \sigma(q_j) := -\sigma(q_{j-1})$. (d) When q_{j-1} and q_j are both locate in background area, we set $\mu(q_j) := \mu(q_{j-1}); \sigma(q_j) := \sigma(q_{j-1})$, external force plays a positive role while expansibility force turns into shrinkage force. In conclusion, detection of the optimal edge curve $B_N^* = \{q_1^*, q_2^*, \dots, q_N^*, q_1^*\}$ of ROI polar image is equivalent to solve the optimization problem:

$$\begin{cases} \min E_{Snake} = \sum_{j=1}^N E(q_j) + E(q_N q_1) \\ s.t. \quad E(q_j) = 0 \end{cases} \quad (7)$$

The solution of problem (7) actually is that we regard target edge detection as searching optimal path.

3. Closed Edge Detection by DP

DP algorithm is an optimization method to deal with multi-step decision process and it is suited to solve the problem (7). For a quasi-circular target trends to be a straight line in polar image, an average filter is cited to detect the potential lines by a convolution operation between the target image and a point spread function (PSF). i.e. $f^* = f \otimes g$, where f represents the target image (shown as Fig. 3(b)), f^* is the filtered image, and g is the PSF. For any point in the filtered image f^* , when its gray-scale value is greater than a pre-set value δ , it is chosen as the starting point of DP. Then we can get the starting point sequence $\{q_j\}$, and investigate the distance d between two adjacent starting points q_i and q_{i+1} . If d is less than a certain threshold, the point (refers to q_i) was removed otherwise reserved.

4. Experiment and Analysis

To illustrate the effectiveness of this algorithm, some images were chosen as the test samples. The parameters were set as following, $\alpha = 0.5, \beta = 0.05, \gamma = 2, \mu = 0.001, \sigma = 0.01$ in this experiment. The performance of this algorithm was evaluated with overlap percentage calculated

by $Overlap = Area(A \cap B) / Area(A \cup B)$, in which A represents the target area and B represents the region after edge extraction, moreover, $Area(X)$ represents the area of region X. When the proposed algorithm was carried out on the images such as bliss image and breast tumor image, the flow chart of detection of edge was shown in Fig. 3 and Fig. 4 from (a) to (f). The results demonstrate that the proposed method achieves satisfactory results.

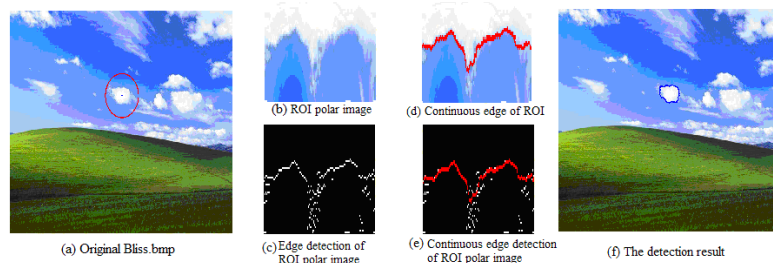


Fig. 3 The flow chart of bliss image by the proposed algorithm

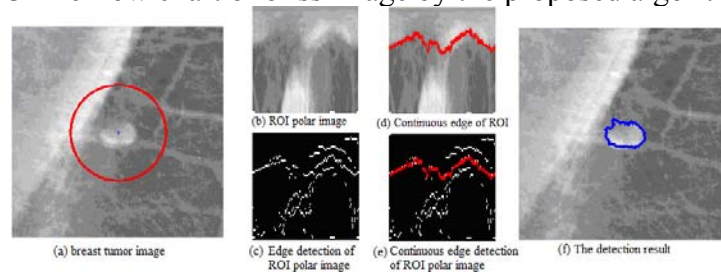


Fig. 4 The flow chart of breast tumor image by the proposed algorithm

Besides, in Fig. 4(a), it can be found that a large area of high-luminance chest rib was involved in ROI which makes the original snake and GVF algorithm trend falling into the local minimum results in a significant deviation between the extracted contour and the real contour.

5. Conclusion

In this paper, we have presented a new method for contours extraction of quasi-circular targets which is based on edge information and dynamic programming. The proposed algorithm has strong anti-noise ability and robustness, and the statistics of overlap percentage is significant.

References

- [1] P. Li, T. Zhang, "Review on active contour model (snake model)". J. of softw., vol.11, pp. 751-757, 2000. (in Chinese).
- [2] D. Cheng, X. Jiang, "Detections of arterial wall in sonographic artery images using dual dynamic programming," IEEE Trans. Info. Technol. in Biomed., vol. 12, pp. 792-799, 2008.
- [3] C. Sun, P. Vallotton, D. Wang, J. Lopez, Y. Ng, and D. James, "Membrane boundary extraction using circular multiple paths," Patt. Recogn., vol. 42, pp. 523-30, April 2009.
- [4] A.A. Amini, T.E. Weymouth, and R.C. Jain, "Using dynamic programming for solving variational problems in vision," IEEE Trans. PAMI. vol. 12, pp. 855-67, 1990.
- [5] H. Zhang, W. Zuo, K. Wang, and D. Zhang, "A snake-based approach to automated segmentation of tongue image using polar edge detector," Int. J. of Imaging Sys. and Technol., vol. 16, pp. 103-112, 2006.
- [6] C. Collewet, "Polar snakes: a fast and robust parametric active contour model," IEEE International Conf. Image Process., pp. 3013-3016, 2009.
- [7] S. Timp, and N. Karssemeijer, "A new 2D segmentation method based on dynamic programming applied to computer aided detection in mammography," Med. Phys., vol. 31, pp. 958-71, 2004.